IOP Publishing New J. Phys. 20 (2018) 063015 https://doi.org/10.1088/1367-2630/aac6f7

New Journal of Physics

The open access journal at the forefront of physics

Deutsche Physikalische Gesellschaft DPG

IOP Institute of Physics

Published in partnership with: Deutsche Physikalische Gesellschaft and the Institute of Physics

OPEN ACCESS

RECEIVED
7 March 2018

REVISED
11 May 2018

ACCEPTED FOR PUBLICATION
22 May 2018

PUBLISHED
12 June 2018

PAPER

Stability of the coexistent superconducting-nematic phase under the presence of intersite interactions

Michał Zegrodnik[1] **and Józef Spałek**[2,3]

[1] Academic Centre for Materials and Nanotechnology, AGH University of Science and Technology, Al. Mickiewicza 30, 30-059 Kraków, Poland

[2] Marian Smoluchowski Institute of Physics, Jagiellonian University, ul. Łojasiewicza 11, 30-348 Kraków, Poland

[3] Author to whom any correspondence should be addressed.

E-mail: michal.zegrodnik@agh.edu.pl **and** jozef.spalek@uj.edu.pl

Keywords: high temperature superconductivity, nematicity, correlated electron systems, t–J–U model, Hubbard model, Gutzwiller wave function, cuprates

Abstract

We analyze the effect of intersite interactions on the stability of the coexisting superconducting-nematic phase (SC+N) within the extended Hubbard and *t–J–U* models on the square lattice. In order to take into account the correlation effects to a proper precision, we use the approach based on the *diagrammatic expansion of the Gutzwiller wave function* (DE-GWF), which goes beyond the *renormalized mean-field theory* (RMFT) in a systematic manner. As a starting point of our analysis we discuss the SC+N phase stability as a function of the intrasite Coulomb repulsion and hole doping for the case of the Hubbard model. Next, we show that the exchange interaction term enhances superconductivity while suppresses the nematicity, whereas the intersite Coulomb repulsion acts in the opposite manner. The competing character of the SC and N phases interplay is clearly visible throughout the analysis. A universal conclusion is that the nematic phase does not survive within the *t–J–U* model for the value of *J* integral typical for the high-T_C cuprates ($J \approx 0.1$ eV). This result is helpful in providing the understanding of the fundamental role of the nodal direction. For the sake of completeness, the effect of the correlated hopping term is also analyzed. Thus the present discussion contains all relevant two-site interactions which appear in the parametrized single-band model of correlated fermions. At the end, the influence of the higher-order terms of the DE on the rotational symmetry breaking is also shown by comparing the DE-GWF results with those of the RMFT.

1. Introduction

The nematic ordering is believed to appear in a number of strongly correlated compounds such as URu_2Si_2 [1], iron-pnictides [2, 3], cuprates [4–6], $Sr_3Ru_2O_7$ [7], as well as quantum Hall systems [8]. Nematicity is characterized by a spontaneous rotational symmetry breaking of the electronic structure, with the preservation of the translational symmetry imposed by the crystal lattice. This condition excludes positional or magnetic orderings such as those appearing in the cases of spin-density-wave (SDW) or charge-density-wave (CDW) phases. However, it has been argued that in the cuprates the CDW phase may be formed through a precursor state which has a nematic character [6]. In some of the copper-based compounds a small distortion of the square lattice makes it difficult to validate the nematic behavior of the electronic wave function, as the C_4 symmetry of the Cu–O planes is already broken by the rhombohedral crystal structure. Nevertheless, in spite of such a small structural distortion, a large anisotropy of various physical properties has been observed [5, 9–12]. This fact, together with the recent research on the La-based cuprate compounds [6, 13] indicate, that the anisotropic character of electronic properties of Cu–O planes is not a trivial consequence of the lattice distortion. Instead, it may be caused by an intrinsic susceptibility towards the nematic order and may be due to the inter-electronic interactions.

For the copper-based materials the appearance of superconducting phase can also be ascribed to the inter-electronic correlation effects. Therefore, the question of the SC and N phases coexistence/competition within typical models referring to strongly correlated systems is worth exploring. According to the mean-field analysis of SC+N appearance for the case of phenomenological model, the two phases compete with each other [14]. Other investigations, which go beyond the mean-field approach, included methods limited to either weak or intermediate interactions [15–18]. The SC+N phase induced solely by strong correlations has been analyzed recently [19] for the case of Hubbard model (with the intrasite repulsion only), by using the *diagrammatic expansion of the Gutzwiller wave function* (DE-GWF) [20–22]. The same method has been applied by us previously to the analysis of the *t–J–U* model, what has lead to a very good quantitative agreement between theory and experiment for the selected principal properties of the pure superconducting phase of the cuprates [23, 24]. Namely, it has been found that the presence of both the exchange *J*-term and the possibility of having a small but non-zero number of double occupancies at the same time, was indispensable to achieve a proper quantitative agreement. One should also note that additional interactions terms, which are frequently omitted, may affect the stability of various correlation-induced phases [25, 26].

Here we use the DE-GWF method in order to carry out a detailed analysis of nematic and superconducting phases coexistence/competition in the presence of all relevant two-site interaction terms, i.e., the antiferromagnetic exchange, the intersite Coulomb repulsion, and the correlated hopping. One of the basic questions here is under which conditions the nematicity can be ignored and hence, the nodal (gapless) direction remains well defined, a feature regarded by us as a fundamental property of the cuprates. The positive answer is shown to result from the competitive in this respect character of the nearest-neighbor exchange and the Hubbard term. To show that the C_4 symmetry breaking presented here is due to inter-electronic effects, we focus mainly on the square lattice structure. Nevertheless, the influence of the preexistent lattice distortion is also discussed. To show that the higher-order terms of our DE are essential to induce the tendency towards the spontaneous C_4 symmetry breaking, we compare the obtained results with those calculated within the *renormalized mean-field theory* (RMFT) [27], a method equivalent to the zeroth order of the DE-GWF expansion [22].

It should be noted that also other phases, which are not studied here, are interesting in the context of the Hubbard-type models. In particular, the magnetically and charge-ordered phases of different kinds have been analyzed over the years [28–34]. Such a study would be additionally motivated by the experimental observation of those states in the copper-based compounds [11, 35–37]. However, the SDW and CDW phases reported in the cuprates are complex and many variants of those phases are discussed, such as bond- and/or site-centered CDW, as well as the *d-wave*, or extended *s-wave* symmetries of the charge modulation, non-zero flux states, stripe or checkerboard CDW, coexistent CDW and SDW phases etc. In our view, a complete set of experimental results, which would describe in detail the SDW and CDW states in the cuprates has not been gathered as yet. Also, very recently, the pair-density-wave phase, for which a modulation of superconducting gap appears, has been observed in BSCCO [38]. Such a state can coexist with the charge-ordered pattern and may have connection with the so-called pseudogap state. One should note that a complete theoretical description of all the above mentioned phases has not been formulated so far and it is not our aim here to provide such a description. Instead, we limit ourselves to the nematic and superconducting phases, without a detailed study of their relative stability with respect to the complex CDW and SDW states. Nonetheless, at the end of the paper we discuss the relation of the N and SC phases to the simplest forms of the magnetic and charge orderings, which we have analyzed previously [26, 39]. Namely, the antiferromagnetic phase, which also appears in the cuprates close to the half-filled situation and the charge ordering with $\mathbf{Q} = (\pi, \pi)$ modulation vector, are briefly touched upon.

The structure of the paper is as follows. In the next section we introduce the *t–J–U–V* model and the DE-GWF method of its solution. In section 3 we discuss the resulting phase diagram and related physical properties comprising the regimes of pure- and coexisting-phases stability. Conclusions are contained in section 4.

2. Model and method

The most general form of the Hamiltonian considered here is given below

$$\hat{\mathcal{H}} = \sum_{\langle ij\rangle\sigma} [t + K(\hat{n}_{i\bar{\sigma}} + \hat{n}_{j\bar{\sigma}})]\hat{c}^{\dagger}_{i\sigma}\hat{c}_{j\sigma} + t' \sum_{\langle\langle ij\rangle\rangle\sigma} \hat{c}^{\dagger}_{i\sigma}\hat{c}_{j\sigma} + J\sum_{\langle ij\rangle} \hat{\mathbf{S}}_i \cdot \hat{\mathbf{S}}_j + U\sum_i \hat{n}_{i\uparrow}\hat{n}_{i\downarrow} + V\sum_{\langle ij\rangle} \hat{n}_i\hat{n}_j. \quad (1)$$

The first two terms contain the single-particle and the correlated hopping ($\sim K$) contributions, respectively, the third term represents the antiferromagnetic exchange interaction, and the last two terms refer to the intra- and intersite Coulomb repulsion. By $\langle ...\rangle$ and $\langle\langle ...\rangle\rangle$ we denote the summations over the nearest neighbors and next-

nearest neighbors, respectively. For $J = K = V \equiv 0$ we obtain the Hubbard model which constitutes the reference point of our analysis of the particular interaction terms and their influence on the SC+N phase. With the increasing $U \rightarrow \infty$ the model reduces to a form of extended t–J model [40].

Strictly speaking, in equation (1) we have ignored the so-called pair-hopping term $\sim J\hat{c}^{\dagger}_{i\uparrow}\hat{c}^{\dagger}_{i\downarrow}\hat{c}_{j\downarrow}\hat{c}_{j\uparrow}$. This term provides a negligible contribution $\sim Jd^4$, where d^2 is the probability of double occupancy. In actual calculations (see below) $d^2 \sim 10^{-2}$, $U \gtrsim 10|t|$ so that, this contribution is of the order of $\sim 10^{-5}|t| < < |E_G| \sim 0.5|t|$. It is also much smaller than the amplitude of the superconducting gap.

In order to take into account the inter-electronic correlations we use the description based on the Gutzwiller-type wave function defined by

$$|\Psi_G\rangle \equiv \hat{P}_G|\Psi_0\rangle, \tag{2}$$

where $|\Psi_0\rangle$ is the non-correlated wave function (to be defined later) and the correlation operator $\hat{P}_G$ is provided below

$$\hat{P}_G \equiv \prod_i \hat{P}_i = \prod_i \sum_{\Gamma} \lambda_{i,\Gamma}|\Gamma\rangle_{ii}\langle\Gamma|, \tag{3}$$

where $\lambda_{i,\Gamma} \in \{\lambda_{i\varnothing}, \lambda_{i\uparrow}, \lambda_{i\downarrow}, \lambda_{id}\}$ are the variational parameters which correspond to four states of the local basis $|\varnothing\rangle_i$, $|\uparrow\rangle_i$, $|\downarrow\rangle_i$, $|\uparrow\downarrow\rangle_i$ at site i, respectively. An important step of the DE-GWF method is the application of the condition [20]

$$\hat{P}_i^2 \equiv 1 + x\hat{d}_i^{\mathrm{HF}}, \tag{4}$$

where x is yet another variational parameter and $\hat{d}_i^{\mathrm{HF}} \equiv \hat{n}_{i\uparrow}^{\mathrm{HF}}\hat{n}_{i\downarrow}^{\mathrm{HF}}$, $\hat{n}_{i\sigma}^{\mathrm{HF}} \equiv \hat{n}_{i\sigma} - n_0$, with $n_0 \equiv \langle\Psi_0|\hat{n}_{i\sigma}|\Psi_0\rangle$. One should note that λ_{Γ} parameters are all functions of x which results in only one variational parameter of the wave function. As it has been shown in [20, 41], condition (4) leads to rapid convergence of the resulting DE with the increasing order in the resultant variational parameter x.

Within this approach, the expectation value in the correlated state from any two local operators, $\hat{o}_i$ and $\hat{o}'_j$, can be expressed in the following manner

$$\langle\Psi_G|\hat{o}_i\hat{o}'_j|\Psi_G\rangle = \sum_{k=0}^{\infty}\frac{x^k}{k!}{\sum_{l_1\ldots l_k}}'\langle\Psi_0|\tilde{o}_i\tilde{o}'_j\,\hat{d}_{l_1\ldots l_k}^{\mathrm{HF}}|\Psi_0\rangle, \tag{5}$$

where $\tilde{o}_i \equiv \hat{P}_i\hat{o}_i\hat{P}_i$, $\tilde{o}'_j \equiv \hat{P}_j\hat{o}'_j\hat{P}_j$, $\hat{d}_{l_1\ldots l_k}^{\mathrm{HF}} \equiv \hat{d}_{l_1}^{\mathrm{HF}}\ldots\hat{d}_{l_k}^{\mathrm{HF}}$, with $\hat{d}_{\varnothing}^{\mathrm{HF}} \equiv 1$. The primed summation has the restrictions $l_p \neq l_{p'}$, $l_p \neq i, j$ for all p and p'.

The averages in the non-correlated state on the right-hand side of equation (5) can be decomposed by the use of the Wick's theorem applied directly in real space and expressed in terms of the correlation functions $P_{ij} \equiv \langle\hat{c}^{\dagger}_{i\sigma}\hat{c}_{j\sigma}\rangle_0$ and $S_{ij} \equiv \langle\hat{c}^{\dagger}_{i\uparrow}\hat{c}^{\dagger}_{j\downarrow}\rangle_0$. Such a procedure allows us to express the ground state energy $\langle\hat{\mathcal{H}}\rangle_G \equiv \langle\Psi_G|\hat{\mathcal{H}}|\Psi_G\rangle/\langle\Psi_G|\Psi_G\rangle$ as a function of P_{ij}, S_{ij}, n_0, and x. It has been shown that the desirable convergence can be achieved by taking the first 4–6 terms of the expansion in x appearing in equation (5) [26, 22]. Here the first 5 terms of the DE (5) have been taken into account when carrying out the calculations. The exemplary expressions for selected terms appearing in the Hamiltonian in the zeroth order expansion are provided in the appendix.

The effective Schrödinger equation can be derived from the minimization condition of the ground state energy functional $\mathcal{F} \equiv \langle\hat{\mathcal{H}}\rangle_G - \mu_G\langle\hat{N}\rangle_G$, where μ_G and $\langle\hat{N}\rangle_G$ are the chemical potential and the total number of particles determined in the state $|\Psi_G\rangle$ [42]. The explicit form the equation is given below

$$\hat{\mathcal{H}}_{\mathrm{eff}}|\Psi_0\rangle = E|\Psi_0\rangle, \tag{6}$$

where the effective single-particle Hamiltonian has the form

$$\hat{\mathcal{H}}_{\mathrm{eff}} = \sum_{ij\sigma} t_{ij}^{\mathrm{eff}}\hat{c}^{\dagger}_{i\sigma}\hat{c}_{j\sigma} + \sum_{ij}(\Delta_{ij}^{\mathrm{eff}}\hat{c}^{\dagger}_{i\uparrow}\hat{c}^{\dagger}_{j\downarrow} + \mathrm{h.c.}), \tag{7}$$

with the effective parameters

$$t_{ij}^{\mathrm{eff}} \equiv \frac{\partial\mathcal{F}}{\partial P_{ij}}, \quad \Delta_{ij}^{\mathrm{eff}} \equiv \frac{\partial\mathcal{F}}{\partial S_{ij}}. \tag{8}$$

It is necessary to introduce the real space cutoff for the parameters P_{ij} and S_{ij}, which are going to be taken into account while executing explicitly the Wick's decomposition of expansion (5). Here, in order to carry out calculations in a reasonable time, the maximum distance has been taken as $R_{\mathrm{max}}^2 = 5a^2$, where a is the lattice constant. The comparison between the situation corresponding to $R_{\mathrm{max}}^2 = 5a^2$ and $R_{\mathrm{max}}^2 = 16a^2$ is provided at the end of the paper and shows that no significant changes are made by increasing R_{max} above the former value.

The self-consistent equations for all the parameters S_{ij} and P_{ij} are derived after transforming the effective Hamiltonian (7) to the reciprocal space. The solution of self-consistent equations is carried out concomitantly

with the minimization over variational parameter x. After calculating P_{ij}, S_{ij}, x, μ_G, and $P_{ii} = n_0$ for a selected set of microscopic parameters (t', K, J, U, V), we can determine the value of the so-called correlated SC gaps $\Delta_{G,ij} \equiv \langle \hat{c}^{\dagger}_{i\uparrow}\hat{c}^{\dagger}_{j\downarrow}\rangle_G$, as well as the correlated hopping averages $P_{G,ij} \equiv \langle \hat{c}^{\dagger}_{i\sigma}\hat{c}_{j\sigma}\rangle_G$.

The *d-wave* gap symmetry is most widely used for the description of high-T_C superconductivity in the cuprates. Here, small higher-order contribution to the bare *d-wave* symmetry (but preserving the zero-gap nodal feature) appear due to the fact that not only nearest pairing averages are included, i.e., those corresponding to atomic sites up to $|\mathbf{R}_{ij}|^2 \equiv |\mathbf{R}_i - \mathbf{R}_j|^2 = 5a^2$ are taken into account. In spite of that, the dominant contribution to the pairing amplitude arises from the nearest-neighbor SC averages: $\Delta^G_{1,0}$, $\Delta^G_{-1,0}$, $\Delta^G_{0,1}$, $\Delta^G_{0,-1}$, where $\Delta^G_{X,Y} \equiv \langle \hat{c}^{\dagger}_{i\uparrow}\hat{c}^{\dagger}_{j\downarrow}\rangle_G$ for $\mathbf{R}_{ij} = (X, Y)a$. For the bare *d-wave* symmetry, the following conditions are fulfilled $\Delta^G_{1,0} = \Delta^G_{-1,0}$, $\Delta^G_{0,1} = \Delta^G_{0,-1}$, and $\Delta^G_{1,0} = -\Delta^G_{0,1}$. However, in general, when the C_4 symmetry is broken, an *s-wave* admixture to the *d-wave* component appears. In such a general situation it is convenient to introduce the *d-wave* and *s-wave* correlated gap parameters, respectively

$$\Delta^G_d = \frac{1}{2}(\Delta^G_{1,0} - \Delta^G_{0,1}),$$
$$\Delta^G_s = \frac{1}{2}(\Delta^G_{1,0} + \Delta^G_{0,1}). \tag{9}$$

Also, since for the nematic phase the (1, 0) and (0, 1) directions are not equivalent, the corresponding hopping averages will also differ and the following parameter characterizing the nematicity can be introduced in the form: $\delta P_G \equiv P^G_{1,0} - P^G_{0,1}$, where $P^G_{X,Y} \equiv \langle \hat{c}^{\dagger}_{i\sigma}\hat{c}_{j\sigma}\rangle_G$, for $\mathbf{R}_{ij} = (X, Y)a$.

In the pure SC phase: $\Delta^G_d \neq 0$, $\Delta^G_s \equiv 0$, and $\delta P_G \equiv 0$, whereas in the coexistent SC+N phase: $\Delta^G_d \neq 0$, $\Delta^G_s \neq 0$, and $\delta P_G \neq 0$. For the case of pure nematic phase (without SC order) one obtains $\Delta^G_d = \Delta^G_s \equiv 0$ and $\delta P^G \neq 0$, whereas for the pure paramagnetic (normal) phase with neither SC nor N we have that $\Delta^G_d = \Delta^G_s \equiv 0$ and $\delta P_G \equiv 0$. In what follows we study systematically the phase diagram involving all the listed phases.

In the DE-GWF method the real space cutoff, $R_{\max}$, defines the number of intersite hopping and superconducting averages (P_{ij} and S_{ij}) that are taken into account in the calculations. Obviously, by using the symmetry relations this number can be additionally reduced. For example, when the C_4 symmetry is conserved, instead of having four different hoppings we have only one ($P_{1,0} = P_{-1,0} = P_{0,1} = P_{0,-1}$). Each average corresponds to one integral equation in the final set of equations that need to be solved numerically. Therefore, when analyzing states with broken symmetry such as the nematic phase we increase the number of integral equations in the problem. For the case of pure *d-wave* state, for which the C_4 symmetry is conserved, the number of equations is equal to 8, whereas for the case of the coexistent superconducting-nematic phase it is equal to 14. Additionally, in the former case one needs to integrate over one quarter of the Brillouin zone and in the latter the integration over twice larger region is required. Also, when allowing for the C_4 symmetry breaking the number of inequivalent diagrams, generated by the Wick's decomposition of the averages in equation (5), significantly increases.

3. Results and discussion

In our analysis we have selected the hopping parameters as $t = -0.35$ eV and $t' = 0.25|t|$ (unless stated otherwise) which are typical for the copper-based compounds. All the energies in the presented results are in units of the nearest-neighbor hopping integral $|t|$. The calculations correspond to the case of square lattice. However, at the end we also discuss the influence of the lattice distortion towards the orthorhombic structure.

First, we analyze the SC and N phase coexistence in the Hubbard model, defined by Hamiltonian (1) with $J = K = V = 0$, for the case of square lattice. These results constitute the reference point for the subsequent analysis focused on the influence of particular two-site terms on the onset of nematicity in the extended models. In figure 1 we plot the phase diagrams on the (U, δ) plane, in which we mark the stability region of the nematic phase coexisting with superconductivity (region labeled by SC+N, with $\Delta^G_s \neq 0$, $\delta P_G \neq 0$, and $\Delta^G_d \neq 0$). As one can see, the appearance of the (1, 0) and (0, 1) directions inequivalence, which manifests itself by the non-zero values of δP_G (shown in figure 1(c)), is accompanied by a concomitant appearance of the *s-wave* component of the SC correlated gap (shown in figure 1(a)). However, the *s-wave* gap amplitude is about two orders of magnitude smaller than that corresponding to the *d-wave* symmetry. For large values of Coulomb repulsion ($U \gtrsim 10$), superconductivity wins over the nematic phase in the underdoped regime and appears in the pure *d-wave* form (region close to $\delta = 0$ labeled by SC in figures 1(a)–(c)). Similar effect has been reproduced in [19], where a small section of the phase diagram is provided. For comparison, in figure 1(d) we show the correlated gap for the case when the nematic phase is not taken into account. In such a situation only *d-wave* component of the SC gap appears and its values are significantly larger as compared to those in the SC+N phase (see

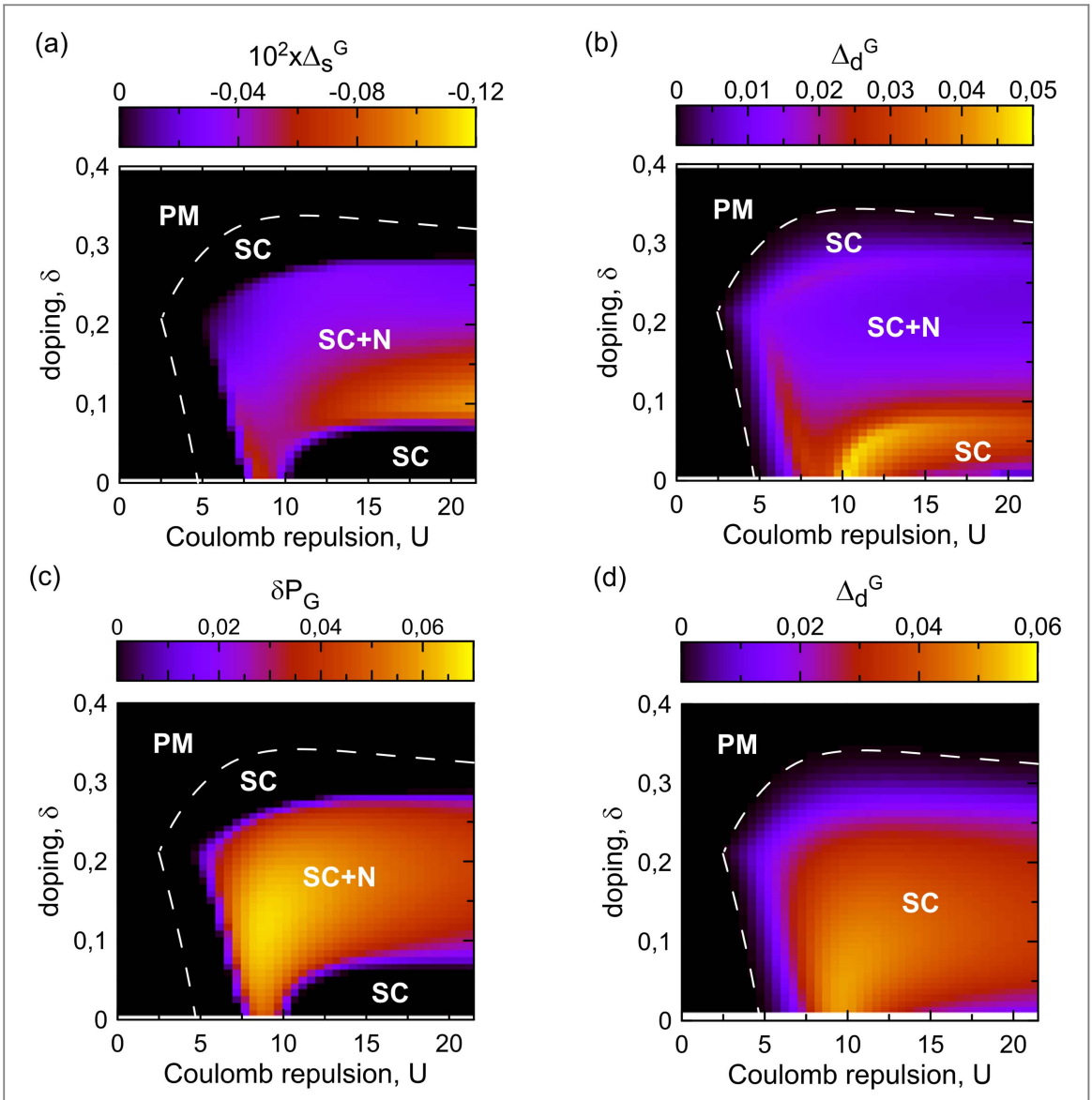

Figure 1. *s-wave* (a) and *d-wave* (b) components of the correlated gap, as well as the nematicity parameter $\delta P_G = P^G_{1,0} - P^G_{0,1}$ (c), all as functions of hole doping δ and the intrasite Coulomb repulsion U. The region with non-zero Δ^G_s and δP_G corresponds to the coexistent SC+N phase, whereas the pure SC phase is characterized by $\Delta^G_s = 0$, $\delta P_G = 0$, and $\Delta^G_d \neq 0$. For the paramagnetic phase (PM): $\Delta^G_s = \delta P_G = \Delta^G_d = 0$. For comparison, in (d) we show the *d-wave* wave correlated gap for the case when the nematic phase is not included in the calculations. The results are for the Hubbard model (with $J = K = V = 0$).

figures 1(b) and (d)). This means that the adjustment of the SC phase to the C_4 symmetry breaking in the coexistent phase leads to the weakening of the *d-wave* superconductivity, which in turn points to the competing character of the SC and N phases interplay.

As shown explicitly in figure 2, the nematic order parameter (δP_G) and the *s-wave* SC gap (Δ^G_s) approach continuously to zero at the doping values, at which the transition to the pure SC phase appear. The first derivative of the energy at the transition points is continuous, which signals the second order transition (see figure 2(d)). Also, in the region labeled by SC+N the coexistent superconducting-nematic phase gives lower energy values than the pure SC phase ($\Delta E = E_{SC+N} - E_{SC} < 0$ show in figure 2(d)). Again, as one can see in figure 2(b), the *d-wave* SC correlated gap in the SC+N phase is reduced in comparison to the pure SC solution.

In figure 3 we analyze the effect of the J-term presence on the C_4 symmetry breaking for two significantly different values of Hubbard U ($U = 11.5$ and $U = 21.5$). With the increasing J the *d-wave* superconductivity is enhanced while the nematicity gets reduced substantially. Above the value of $J \approx 0.15$ the latter is completely destroyed leaving only the pure SC phase without any *s-wave* component of the gap. For larger U values (figures (b), (d), (f)) the effect of N phase suppression is even stronger. As a result, the nematicity is already destroyed for the set of parameters, for which a semi-quantitative agreement between theory and experiment has been obtained in [23] with respect to high-T_C superconductivity in the copper-based compounds ($t = -0.35$ eV, $t' = 0.25|t|$, $U = 22$, $J = 0.25|t|$). Hence, the latter results are not affected by the *s-wave* SC gap component

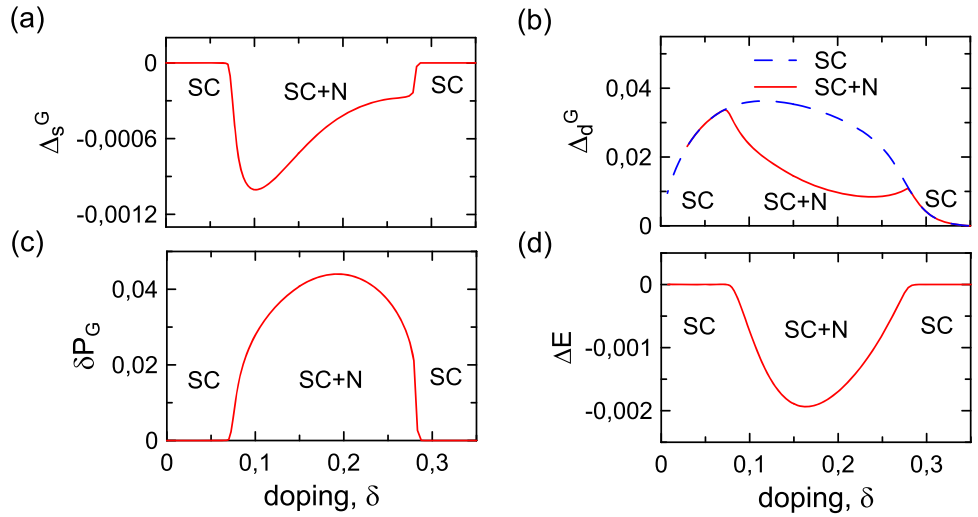

Figure 2. *s-wave* (a) and *d-wave* (b) components of the correlated gap, the nematicity parameter $\delta P_G = P^G_{1,0} - P^G_{0,1}$ (c), as well as the energy difference between the pure superconducting solution and the coexistent superconducting-nematic solution ($\Delta E = E_{SC+N} - E_{SC}$), all as functions of hole doping δ and for the value $U = 21.5$. In (b) we show the *d-wave* SC gap for the case of the SC+N (red solid line) and pure SC (blue dashed line) phases.

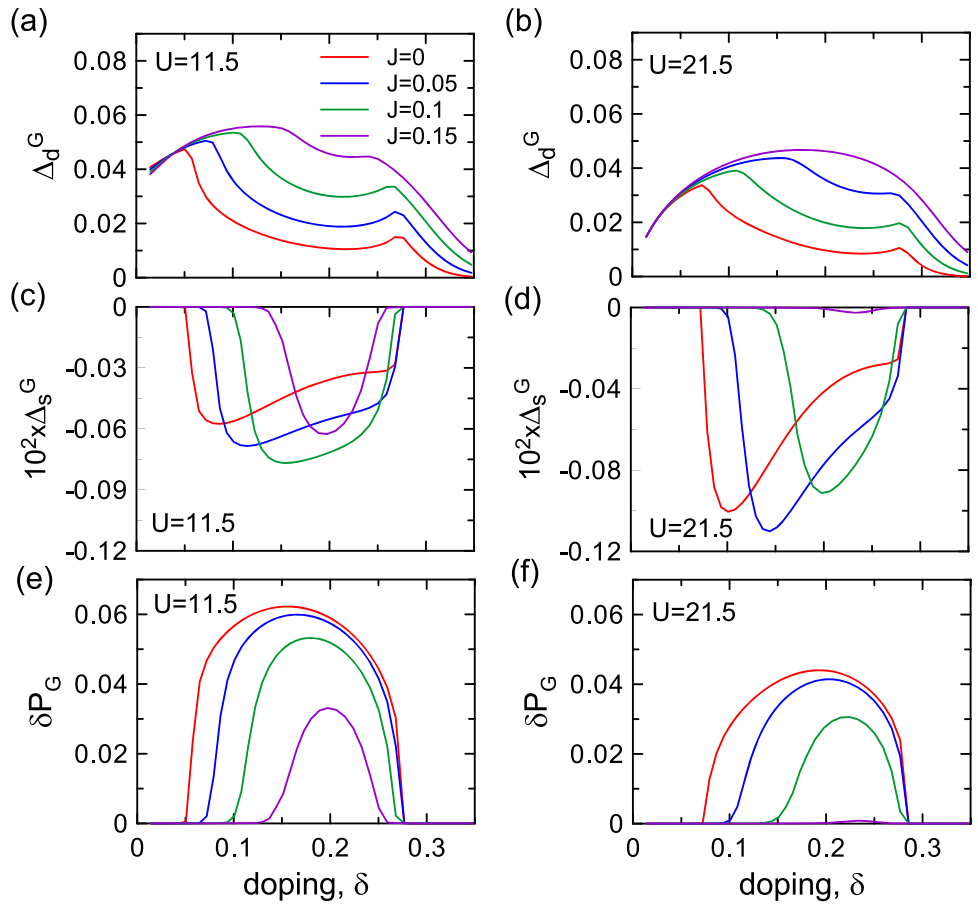

Figure 3. *d-wave* (a), (b) and *s-wave* (c), (d) components of the correlated gap, as well as the nematicity parameter $\delta P_G = P^G_{1,0} - P^G_{0,1}$ (e), (f), all versus hole doping for selected values of the J and U parameters. Note that for large U and with the increasing J the nematicity disappears. The results are for $V = K = 0$.

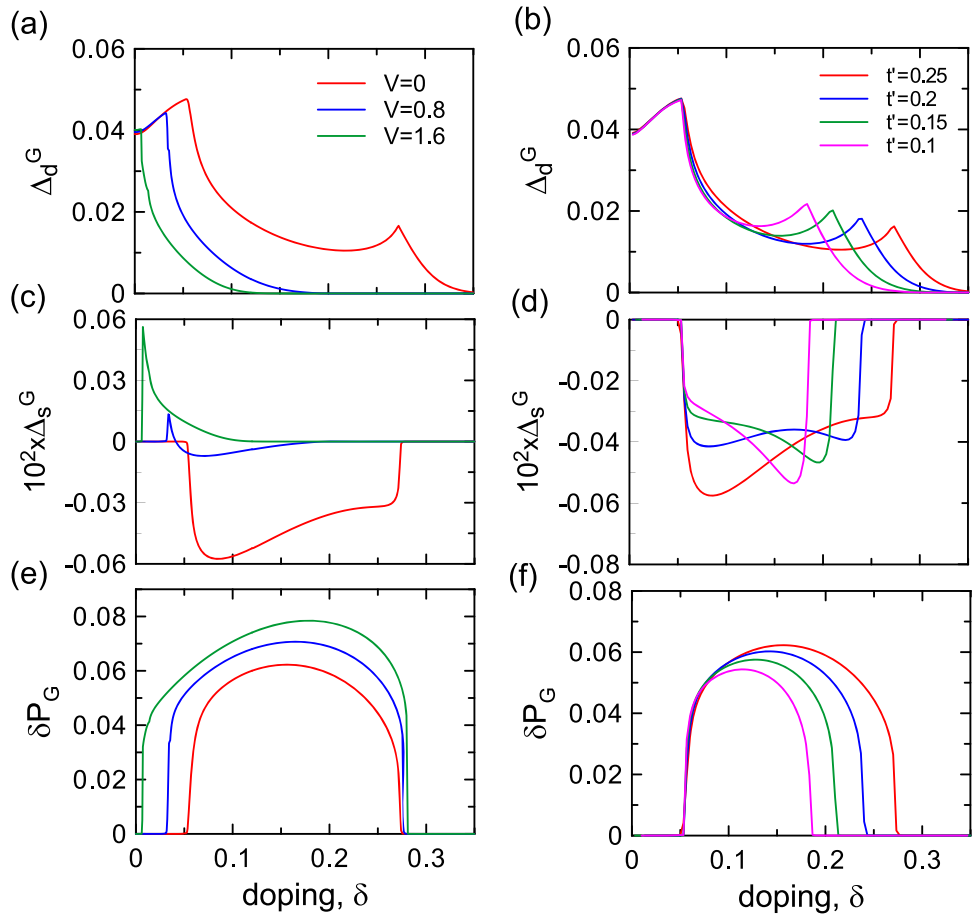

Figure 4. *d-wave* (a), (b) and *s-wave* (c), (d) components of the correlated gap, as well as the nematicity parameter $\delta P_G = P^G_{1,0} - P^G_{0,1}$ (e), (f), all as functions of hole doping for selected values of V and t' and for $J = K = 0$, $U = 11.5$. Note that with the increasing V the nematicity is enhanced (see (e)), whereas the SC phase is suppressed (see (a)). Figures (a), (c), (e) correspond to $t' = 0.25$, while figures (b), (d), (f) correspond to the $V = 0$ case.

appearance which would be destructive for the nodal ($\Gamma - M$) direction presence observed universally in the cuprates.

The intersite Coulomb repulsion term acts in the opposite manner than the J-term. Namely, it suppresses the pairing (see figures 4(a) and (c)) and enhances the nematicity (see figure 4(e)). Therefore, in the model with both J- and V-terms included, the competition between N and SC phases is determined by the interrelation of both these factors. As a consequence, the SC+N phase can be sustained for values of J typical for the cuprates ($J \approx 0.3$) when sufficiently strong intersite Coulomb integral is considered. In figure 5 we present such a situation which represents the t–J–U–V model case. However, here the nematicity appears in the overdoped regime which would be against the experimental findings for the cuprates.

For the sake of completeness we also analyze the influence of electronic structure details on the SC+N phase stability. Namely, in figures 4(b), (d), and (f) we exhibit the doping dependence of the correlated gap components and the nematicity factor for selected values of the next-nearest-neighbor hopping integral t'. As one can see, with the decreasing t' value the stability region of the SC+N phase narrows down. However, the lower critical concentration for the nematicity onset is not affected and is close to $\delta = 0.05$ (see figure 4(f)), which is similar to the upper critical concentration for the AF phase disappearance observed in experiments on the cuprates. This result differs from the one obtained recently in [16], where it was shown that the lower critical concentration for the N phase appearance is moving together with the filling value (tuned by t') which corresponds to the van Hove singularity. This discrepancy can be caused by the differences in details of the two approaches. Namely, in the above mentioned work the fluctuation exchange approximation combined with the dynamical mean-field theory (FLEX+DMFT) method has been used in the intermediate correlations regime ($U = 4$) and at higher temperature $\beta|t| = 20$.

The off-diagonal elements of the Coulomb interaction between the nearest neighboring lattice sites $\langle i, j\rangle$, with the corresponding two-site integral $K_{ij} \equiv \langle \mathbf{ii}|V(\mathbf{r} - \mathbf{r}')|\mathbf{ij}\rangle$ introduce the so-called correlated hopping term, which also has been studied by us [25]. In figure 6 we show the parameters which characterize the SC+N phase as functions of both hole doping δ and the correlated hopping integral K. As one can see, the influence is

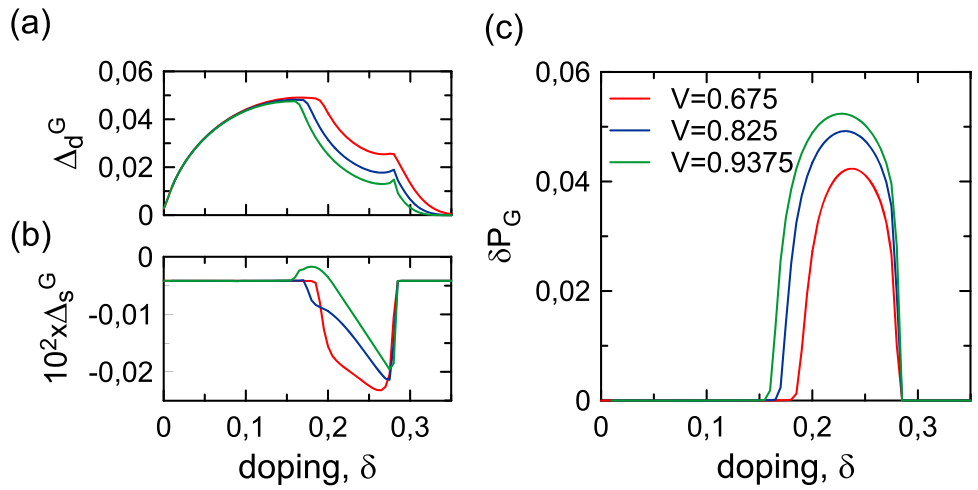

Figure 5. *d-wave* (a) and *s-wave* (b) components of the correlated gap, as well as the nematicity parameter $\delta P_G = P^G_{1,0} - P^G_{0,1}$ (c), all as a function of hole doping for selected values of intersite Coulomb repulsion integral V and for $U = 20, J = 0.3$.

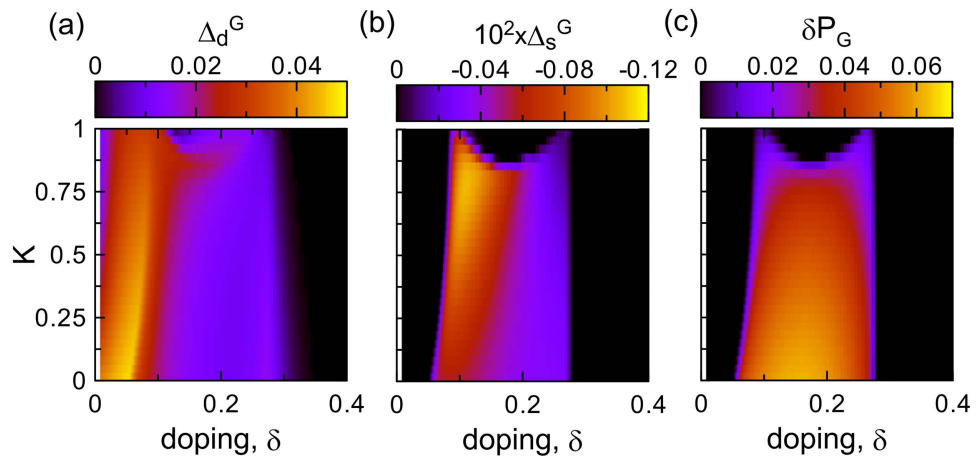

Figure 6. *d-wave* (a), and *s-wave* (b) components of the correlated gap, as well as the nematicity parameter (c), all as functions of hole doping and correlated hopping integral K, for $U = 11.5$ and $J = V = 0$.

not significant up to the values of $K \approx 1$, close to which the nematicity is destroyed and the SC order is being reduced.

Within the present approach the appearance of the nematic phase is not induced by any straightforward mechanism such as the lattice distortion. Instead, the C_4 symmetry of the electronic wave function is broken spontaneously for high enough values of Hubbard U. It should be noted that in order to obtain the effect of a spontaneous C_4 symmetry breaking one should apply approach, which captures the small Fermi-surface deformations. This is probably the reason why, the methods such as the cluster DMFT or cluster Monte-Carlo [43, 44], which suffer from the finite-size scaling effects, lead to the nematic solutions only for a distored structure. On the other hand, by adjoining the FLEX approach with DMFT one avoids the finite-size scaling and the spontaneously appearing nematicity for the square lattice case is reproduced in a similar manner as our DE-GWF analysis [16]. The susceptibility towards the nematic Fermi-surface deformations can be explained in the weak-coupling regime by the use of perturbation theory [45], where also the competing character of the nematic and SC phases is reported. As shown there, a negative contribution to the self-energy appears, which corresponds to the opening of the Fermi-surface close the Lifshitz transition. Since the corresponding term in the perturbation expansion, which drives the symmetry breaking is proportional to U^2 it is understandable that the nematicity appears when U is not too small, which in turn is consistent with our results (see figure 1).

Since often small orthorombic distortion of the Cu–O lattice appears in the cuprates, in figure 7 we provide the results also for the distorted case. The lattice structure is changed by tuning the $t_{0,1}/t_{1,0}$ ratio and the next-nearest-neighbor hopping is set to $t' = 0.25\sqrt{t_{1,0}^2 + t_{0,1}^2}/\sqrt{2}\,|t|$, so that in the case $t_{0,1} = t_{1,0} = t$ we obtain the

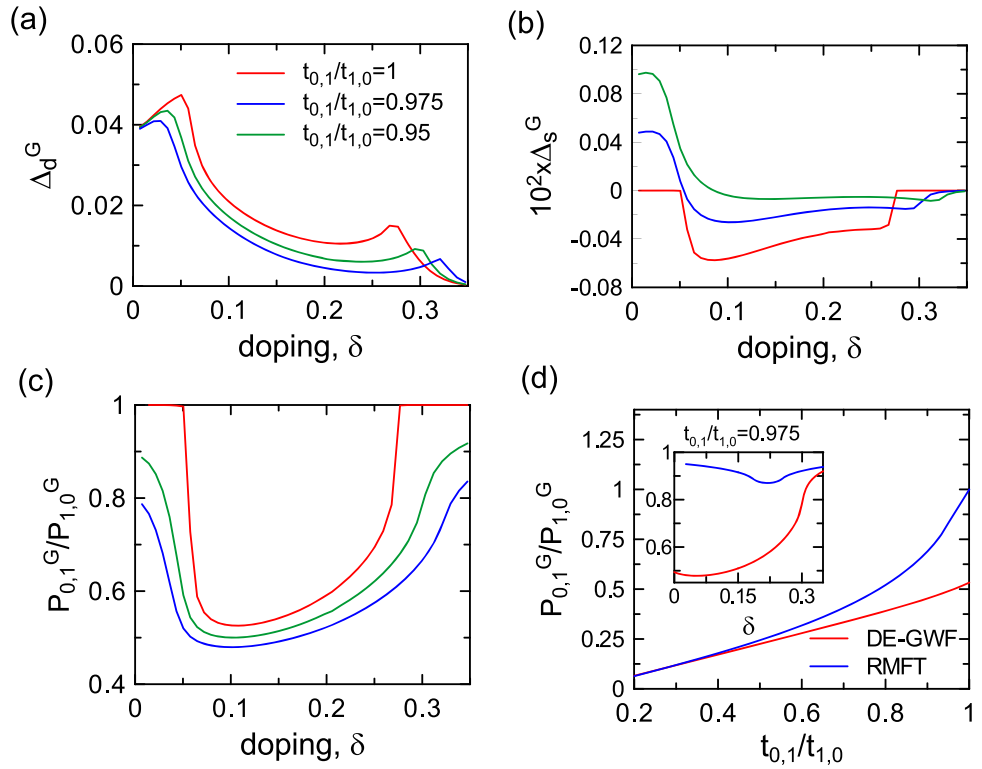

Figure 7. *d-wave* (a), and *s-wave* (b), components of the correlated gap, as well as $P^G_{0,1}/P^G_{1,0}$ (c) all as a function of hole doping for different values of the lattice distortion rate, $t_{0,1}/t_{0,1}$. For $t_{0,1}/t_{1,0} < 1$ the lattice distortion is introduced which enhances nematicity and suppresses *d-wave* superconductivity. In (d) we show $P^G_{0,1}/P^G_{1,0}$ for the case of pure nematic phase for $\delta = 0.1$ as a function of the lattice distortion rate for the case of DE-GWF and RMFT calculations. The inset shows the doping dependence of $P^G_{0,1}/P^G_{1,0}$ for the case of pure nematic phase for the selected value of $t_{0,1}/t_{1,0} = 0.975$. The results are for the Hubbard model ($J = V = K = 0$) with $U = 11.5$.

condition used for the square lattice with $t' = 0.25\ |t|$. One can see from figure 7 that when $t_{0,1}/t_{1,0} \neq 1$, the *d-wave* gap is decreased mainly in the region of SC+N phase stability and the *s-wave* gap component changes sign (see figures 7(a) and (b)). In figures 7(c) and (d) we show how the anisotropy in the hopping integrals affects that of the hopping averages, $P^G_{0,1}/P^G_{1,0}$. As one can see, in the doping range $\delta \gtrsim 0.1$, $\delta \lesssim 0.3$, for a very small lattice anisotropy ($t_{0,1}/t_{1,0} \approx 0.95$, $t_{0,1}/t_{1,0} \approx 0.975$) we obtain a substantial anisotropy of the hopping averages ($P^G_{0,1}/P^G_{1,0} \approx 0.6$).

In figure 7(d), we provide the comparison between the DE-GWF and RMFT methods [27]. Since within the RMFT approach no stability of the SC phase is obtained in the Hubbard model, we compare the two methods limiting to the pure nematic phase only. As one can see, for the case of square lattice ($t_{0,1}/t_{1,0} = 1$), no nematic behavior ($P^G_{0,1}/P^G_{1,0} = 1$) is obtained according to the RMFT method, whereas within the DE-GWF approach the anisotropic behavior of the electronic system is sustained. Also, as shown in the inset to figure 7(d), in RMFT we obtain $P^G_{0,1}/P^G_{1,0} \approx t_{0,1}/t_{1,0}$ in the whole doping range, while the DE-GWF approach leads to a large enhancement of the electronic anisotropy for $\delta \lesssim 0.3$. Such result shows the significance of the higher-order terms of the DE (5) on the C_4 symmetry breaking. As shown before [22] the RMFT method is equivalent to the zeroth order DE-GWF approach. It should be noted that a large nematic anisotropy, induced by a small orthorombic distortion, has been also reported in [43, 44], where the DMFT and dynamical cluster Monte-Carlo methods have been used, respectively. For the case of no SC ordering those studies have shown an increasing nematic anisotropy with decreasing doping, which is consistent with our DE-GWF result presented in the inset of figure 7(d) (red solid line). When the correlation-induced pairing is taken into account the dome-like behavior of the nematic order parameter appears for both the distorted system and the square lattice case (see figures 7(c) and 2(c), respectively). It is caused by the SC phase, which suppresses the nematic state for the low doping values. Similar dome-like behavior of the nematicity has been presented recently both experimentally [6] and theoretically [16, 19].

Additionally, in figure 8 we provide the results for the case of the *t–J–U* model with the preexisting lattice distortion. As we could see earlier (see figure 3) the inclusion of the exchange term $\sim J$ has a destructive influence on the nematicity and for the model parameters corresponding to the cuprates ($J \approx 0.3$) the spontaneous nematicity is already suppressed (see figure 3). However, the nematic anisotropy is brought back for the distorted system. For the relatively large value of the J parameter, the effect of the lattice distortion on the *d-wave*

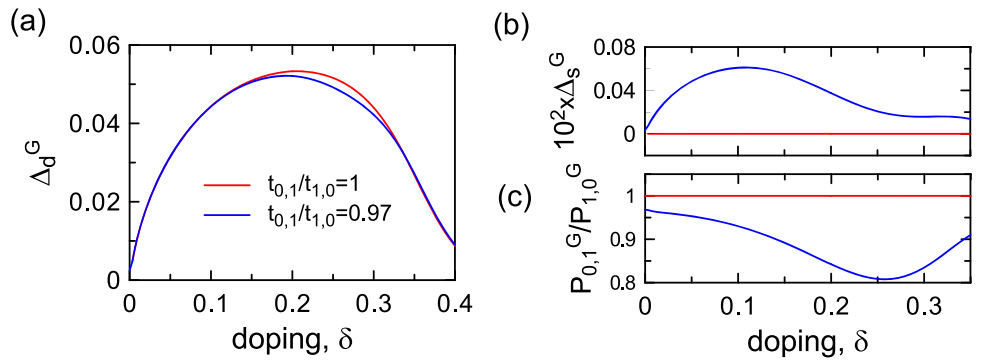

Figure 8. *d-wave* (a), and *s-wave* (b), components of the correlated gap, as well as $P_{0,1}^G/P_{1,0}^G$ (c); all as a function of hole doping for the case of *t–J–U* model without (red solid line) and with (blue solid line) the lattice distortion. The results correspond to $U = 21.5$, $J = 0.3$.

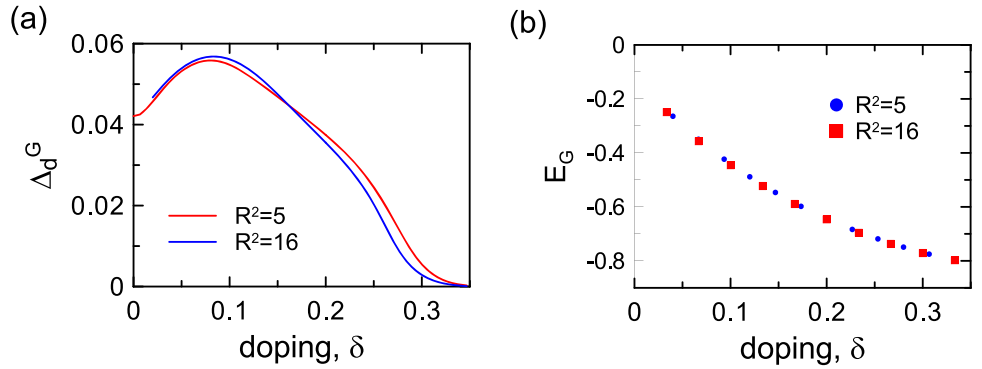

Figure 9. (a) The *d-wave* gap and the ground state energy as functions of doping for two different real space cut-offs $R_{\max}^2 = 5$ and $R_{\max}^2 = 16$ for the case of the Hubbard model with $U = 21.5$. The results have been obtained within the third order of the diagrammatic expansion (5).

SC gap is very small (figure 8(a)). Nevertheless, the value of $P_{0,1}^G/P_{1,0}^G$ is significantly smaller than the $t_{0,1}/t_{1,0}$ ratio which means that the tendency towards C_4 symmetry breaking is still substantial (figure 8(a)).

To check the accuracy of our results, we have plotted in figure 9 the superconducting gap components Δ_d^G, Δ_s^G, as well as the ground state energy E_G, for the two preselected values of the real space cutoff $R_{\max}^2 = 5a^2$ and $R_{\max}^2 = 16a^2$. We see that they are practically the same, what justifies the choice of the smaller value, in turn shortening appreciatively the computing time.

4. Summary and conclusions

This paper is a continuation of our detailed studies of high-T_C SC within the extended *t–J* (or alternative extended Hubbard) model treated within the DE-GWF, implemented in two dimensions, that goes beyond the renormalized mean-field theory in a systematic manner [23–26]. Explicitly, we have analyzed the effect of all the relevant intersite interaction terms on the coexistence of the superconducting (SC) and nematic (N) phases within that method. As a starting point of our analysis we have determined the stability range of the coexistent phase on the (δ, U) plane for the case of Hubbard model. The coexistent SC+N phase appears for high enough values of the Coulomb repulsion ($U \gtrsim 6$) and in a wide doping range (see figure 1). Due to the C_4 symmetry breaking, the *d-wave* pairing amplitude is suppressed and a small *s-wave* component of the SC gap appears in the SC+N phase (see[12, 19]). This signals a competing character of the SC and N phases interplay. The SC/N competition has been also reported by other authors. Moreover, the appearance of the *s-wave* SC component with the onset of nematicity, in addition to the dominant *d-wave* SC, hampers the fundamental gapless character of the nodal direction. Fortunately, the *s-wave* amplitude is about two orders of magnitude smaller than that of the *d-wave*.

For the case of the extended (*t–J–U–V*) model the competition between SC and N is determined by both the exchange interaction and the intersite Coulomb repulsion terms Namely, the *J*-term enhances SC and

suppresses nematicity, whereas for the V-term the opposite is true (see figures 3 and 4(a), (c), (d)). According to our analysis of the t–J–U model, the nematicity survives up to $J \approx 0.15$, what means that the SC+N phase is already destroyed for the parameter set, for which a good agreement between theory and experiment has been achieved for the copper-based superconductors [23]. Hence, in such a situation the *s-wave* gap component is absent (i.e., only the pure *d-wave* SC survives) and the nodal SC character is reinstated. Nevertheless, by adding the V-term to the t–J–U model, one could still sustain the stability of the SC+N phase for the values of $J \approx 0.3$, typical for the cuprates. This means that a detailed analysis of the situation requires going beyond either Hubbard or t–J models, as shown on this example.

Our analysis of the effect of electronic structure details on the SC+N coexistent phase have shown that there is no influence of the van Hove singularity position on the lower critical doping for the coexistent phase onset. For all the considered t' values the lower critical doping remains almost constant and equal to $\delta_c \approx 0.05$, the value close to that, below which the antiferromagnetic phase appears in the cuprates. This result differs with that presented in [16], where the FLEX+DMFT method has been used. However, as mentioned earlier, the results obtained within the latter method are limited to relatively small Hubbard model U values.

The influence of the correlated hopping term on the SC+N phase is not significant up to the value $K \approx 1$, where the nematicity is destroyed and the *d-wave* gap is suppressed (see figure 6).

As could be expected, the assumed from the start distortion of the lattice induces anisotropy of the electronic properties in the whole doping range. However, a substantial increase of the electronic anisotropy is obtained within the region $\delta \approx 0.05 - 0.3$ for the case of the coexistent SC+N phase (see figure 7(c)). Similar result occurs for the pure N phase, however here, the nematic order permeter rises with decreasing hole doping down to the half-filled situation and no dome-like shape is observed (see inset to figure 7(d)). Such results brings into mind the experimental data for the cuprates, where a very small structural distortion also leads to a large effect for selected physical properties [5, 9–11]. The latter result is not reproduced within the RMFT method, where we obtain $P^G_{0,1}/P^G_{1,0} \approx t_{0,1}/t_{1,0}$ in the whole doping range. Moreover, within the RMFT, no spontaneous C_4 symmetry breaking appears for the case of square lattice (see figure 7(d)). This, in turn, demonstrates that the correlation effects taken, into account in the higher-order of the DE-GWF approach, are responsible for the nematic phase appearance for the square lattice case.

It would be interesting to investigate within the present approach whether the susceptibility towards the C_4-symmetry breaking of the electronic system can also induce the orthorhombic crystal distortion. In order to take into account the subtle interplay between the electronic system and the lattice structure, one would have to calculate the hopping integrals in an *ab initio* fashion, instead of treating them as model parameters as here. Such an analysis could be carried out by combining the DE-GWF method(or other method dedicated for the correlated systems [46]) with e.g. the EDABI [47–49] approach. Moreover, such a method could also be used to analyze theoretically the interplay between the unconventional superconductivity and lattice distortion, which is observed in the copper-based compounds [50].

As already stated in the Introduction, here we have not carried out a detailed analysis of the relative stability of the nematic and superconducting phases against the CDW and SDW states. Such a study would be interesting due to the fact that the latter two are observed in the underdoped samples of the cuprates. Nevertheless, in our earlier papers we have analyzed the appearance of the two simplest forms of magnetic and charge orderings within the t–J–U model. Namely, in [26, 39] the antiferromagnetic and the (π, π)-charge-ordered phases have been considered. According to the results presented in [39], the value of upper critical doping for the disappearance of the antiferromagnetic phase is $\delta \sim 0.01$ which is close to the experimental one. Within other theoretical considerations, a similar value has been obtained for the case of the Hubbard model [51, 52]. As we have shown here, in the strongly correlated regime ($U \gtrsim 10$) a coexistent superconducting-nematic phase appears above that value in the considered types of models (except for the situation corresponding to relatively large values of the intersite Coulomb repulsion, V). The (π, π)-charge-ordered phase has been studied in [26] and according to those results charge ordering becomes stable for relatively large values of hole doping ($\delta \approx 0.5$). As one can see, from the present paper the SC+N phase appears below that doping range. With that being said, we can conclude that the nematicity and the two mentioned forms of magnetic and charge ordering appear in different regions of the phase diagram and hence the competition between them does not occur. Nevertheless, the situation can be significantly different for the case of more sophisticated forms of magnetic and charge ordering. As shown in [26] changing the modulation vector from $\mathbf{Q} = (\pi, \pi)$ to $\mathbf{Q} = (2\pi/3, \pi)$, results in significant change in the stability region. The inclusion of various forms of the CDW state within the DE-GWF approach requires a separate analysis. We should see progress along these lines in the near future.

Acknowledgments

MZ acknowledges the financial support from the Ministry of Science and Higher Education of Poland. JS acknowledges the financial support through the Grant MAESTRO, No. DEC-2012/04/A/ST3/00342 from the National Science Centre (NCN) of Poland.

Appendix. Zeroth order expansion

Below we show examples of the zeroth order expansion (5) for selected expressions which are useful in calculating the expectation value of Hamiltonian (1) in the correlated state (2)

$$\langle\Psi_G|\hat{c}^{\dagger}_{i\sigma}\hat{c}_{j\sigma}|\Psi_G\rangle = q^2\ \langle\hat{c}^{\dagger}_{i\sigma}\hat{c}_{j\sigma}\rangle_0 + q\alpha\ \langle\hat{c}^{\dagger}_{i\sigma}\hat{n}^{\mathrm{HF}}_{j\bar{\sigma}}\hat{c}_{j\sigma}\rangle_0 + \alpha q\ \langle\hat{n}^{\mathrm{HF}}_{i\bar{\sigma}}\hat{c}^{\dagger}_{i\sigma}\hat{c}_{j\sigma}\rangle_0 + \alpha^2\ \langle\hat{n}^{\mathrm{HF}}_{i\bar{\sigma}}\hat{c}^{\dagger}_{i\sigma}\hat{n}^{\mathrm{HF}}_{j\bar{\sigma}}\hat{c}_{j\sigma}\rangle_0, \tag{A.1}$$

$$\langle\Psi_G|\hat{\mathbf{S}}_i\hat{\mathbf{S}}_j|\Psi_G\rangle = \lambda_s^4\langle\hat{\mathbf{S}}_i\hat{\mathbf{S}}_j\rangle_0, \tag{A.2}$$

$$\langle\Psi_G|\hat{n}_{i\uparrow}\hat{n}_{i\downarrow}|\Psi_G\rangle = \lambda_d^2\langle\hat{n}_{i\uparrow}\hat{n}_{i\downarrow}\rangle_0, \tag{A.3}$$

where

$$q = \lambda_s(\lambda_d n_0 + \lambda_{\varnothing}(1 - n_0)),\ \alpha = \lambda_s(\lambda_d - \lambda_{\varnothing}), \tag{A.4}$$

and $\lambda_{\uparrow} = \lambda_{i\downarrow} \equiv \lambda_s$ (for the spin-isotropic case). As already said in section II all the λ parameters can be expressed with the use of x

$$\lambda_d^2 = 1 + x(1 - n_0)^2,\ \lambda_s^2 = 1 - xn + 0(1 - n_0),\ \lambda_{\varnothing}^2 = 1 + xn_0^2. \tag{A.5}$$

If we additionally neglect the terms with the α coefficient in (A.1), we would obtain the expressions known from the RMFT where the correlated averages are equal to their non-correlated correspondents premultiplied by the renormalization factors (for the case of hopping that factor would be equal to q^2).

ORCID iDs

Józef Spałek https://orcid.org/0000-0001-5801-5174

References

[1] Okazaki R, Shibauchi T, Shi H J, Haga Y, Matsuda T D, Yamamoto E, Onuki Y, Ikeda H and Matsuda Y 2011 *Science* **331** 439
[2] Chu J-H, Kuo H-H, Analytis J G and Fisher I R 2012 *Science* **337** 710
[3] Fernandes R M, Chubukov A V and Schmalian J 2014 *Nat. Phys.* **10** 97
[4] Keimer B, Kivelson S A, Norman M R, Uchida S and Zaanen J 2015 *Nature* **518** 179
[5] Lawler M J *et al* 2010 *Nature* **466** 347
[6] Pelc D *et al* 2016 *Nat. Commun.* **7** 12775
[7] Borzi R A, Grigera S A, Farrell J, Perry R S, Lister S J S, Lee S L, Tennant D A, Maeno Y and Mackenzie A P 2007 *Science* **315** 214
[8] Lilly M P, Cooper K B, Eisenstein J P, Pfeiffer L N and West K W 1999 *Phys. Rev. Lett.* **82** 394
[9] Ando Y, Segawa K, Komiya S and Lavrov A N 2002 *Phys. Rev. Lett.* **88** 137005
[10] Daou R *et al* 2010 *Nature* **463** 519
[11] Hinkov V, Haug D, Fauqué B, Bourges P, Sidis Y, Ivanov A, Bernhard C, Lin C T and Keimer B 2008 *Science* **319** 597
[12] Betouras J and Joynt R 1995 *Europhys. Lett.* **31** 119
[13] Achkar A J *et al* 2016 *Science* **351** 576
[14] Yamase H and Metzner W 2007 *Phys. Rev.* B **75** 155117
[15] Neumayr A and Metzner W 2003 *Phys. Rev.* B **67** 035112
[16] Kitatani M, Tsuji N and Aoki H 2017 *Phys. Rev.* B **95** 075109
[17] Honerkamp C, Salmhofer M and Rice T M 2002 *Eur. Phys. J.* B **27** 127
[18] Hankevych C, Grote I and Wegner F 2002 *Phys. Rev.* B **66** 094516
[19] Kaczmarczyk J, Schickling T and Bünemann J 2016 *Phys. Rev.* B **94** 085152
[20] Bünemann J, Schickling T and Gebhard F 2012 *Europhys. Lett.* **98** 27006
[21] Kaczmarczyk J, Bünemann J and Spałek J 2013 *Phys. Rev.* B **88** 115127
[22] Kaczmarczyk J, Bünemann J and Spałek J 2014 *New J. Phys.* **16** 073018
[23] Spałek J, Zegrodnik M and Kaczmarczyk J 2017 *Phys. Rev.* B **95** 024506
[24] Zegrodnik M and Spałek J 2017 *Phys. Rev.* B **95** 024507
[25] Zegrodnik M and Spałek J 2017 *Phys. Rev.* B **96** 054511
[26] Abram M, Zegrodnik M and Spałek J 2017 *J. Phys.: Condens. Matter* **29** 365602
[27] Edegger B, Muthukumar V N and Gros C 2007 *Adv. Phys.* **56** 927–1003
[28] Allais A *et al* 2014 *Phys. Rev.* B **90** 155114
[29] Yang K-Y *et al* 2009 *New J. Phys.* **11** 055053
[30] Tu W-L and Lee T-K 2016 *Sci. Rep.* **6** 18675
[31] Faye J P L and Sénéchal D 2017 *Phys. Rev.* B **95** 115127
[32] Corboz P, Rice T M and Troyer M 2014 *Phys. Rev.* B **113** 046402
[33] White S R and Scalpino D J 2004 *Phys. Rev.* B **70** 220506(R)

[34] Loder F, Graser S, Schmid M, Kampf A P and Kopp T 2011 *New J. Phys.* **13** 113037
[35] Comin R *et al* 2015 *Nat. Mater.* **14** 796
[36] Tabis W *et al* 2014 *Nat. Commun.* **5** 5875
[37] Hucker M *et al* 2014 *Phys. Rev.* B **90** 054514
[38] Hamidian M H *et al* 2016 *Nature* **532** 343
[39] Abram M, Kaczmarczyk J, Jędrak J and Spałek J 2013 *Phys. Rev.* B **88** 094502
[40] Spałek J, Oleś A M and Chao K A 1981 *Phys. Status Solidi* b **108** 329
[41] Gebhard F 1990 *Phys. Rev.* B **41** 9452
[42] Schickling T, Bünemann J, Gebhard F and Weber W 2014 *New J. Phys.* **16** 093034
[43] Okamoto S, Sénéchal D, Civelli M and Tremblay A-M S 2010 *Phys. Rev.* B **82** 180511(R)
[44] Su S-Q and Maier T A 2011 *Phys. Rev.* B **84** 220506(R)
[45] Slizovskiy S, Rodriguez-Lopez P and Betouras J J 2018 arXiv:1803.00675
[46] LeBlanc J P F *et al* 2015 *Phys. Rev.* X **5** 041041
[47] Biborski A, Kądzielawa A P and Spałek J 2015 *Comput. Phys. Commun.* **197** 7
[48] Kądzielawa A P, Biborski A and Spałek J 2015 *Phys. Rev.* B **92** 161101(R)
[49] Biborski A, Kądzielawa A P and Spałek J 2017 *Phys. Rev.* B **96** 085101
[50] Horn P M, Keane D T, Held G A, Jordan-Sweet J L, Kaiser D L, Holtzberg F and Rice T M 1987 *Phys. Rev. Lett.* **59** 2772
[51] Spanu L, Lugas M, Becca F and Sorella S 2008 *Phys. Rev.* B **77** 024510
[52] Pathak S, Shenoy V B, Randeria M and Trivedi N 2009 *Phys. Rev. Lett.* **102** 027002